Structure of Chlorophyll *a* Dimers in Solution from Proton Magnetic Resonance and Visible Absorption Spectroscopy[1]

A. D. Trifunac and J. J. Katz*

Contribution from the Chemistry Division, Argonne National Laboratory, Argonne, Illinois 60439. *Received February 15, 1974*

Abstract: A lanthanide-induced shift (LIS) study of chlorophyll *a* in carbon tetrachloride and benzene indicates that the dimer (Chl_2) present in these solutions experiences a change in conformation when the shift reagent is added. This interpretation of the consequences of shift reagent binding is supported by an examination of the visible absorption spectra of the chlorophyll–shift reagent adduct by computer deconvolution techniques. In a related LIS study, the structures of the methyl pheophorbide *a* and methyl bacteriopheophorbide *a* shift reagent complexes have been established.

An understanding in detail of the way in which light energy is manifested as chemical oxidation and reduction potential is the focus of much current endeavor in photosynthesis research. It is generally agreed that chlorophyll is intimately involved as the photoacceptor in the light conversion process, largely because of the similarity between the visible absorption spectrum of chlorophyll and the action spectrum of photosynthesis in green plants.[2] Chlorophyll *a* (Chl *a*), the most common of chlorophylls, is present in every organism that evolves molecular oxygen by photosynthesis, and is the chief subject of discussion in the present communication.

Spectroscopic studies of Chl *a* establish it as a molecule with both electron donor and acceptor properties.[3-10] The ring V keto C=O group (Figure 1) can function as donor, while the central Mg atom possesses strong acceptor properties. In essence, the central Mg atom with coordination number 4 is coordinatively unsaturated, and, as a consequence, an electron donor group must always be present in at least one of the Mg axial positions.[11] In the absence of extraneous nucleophiles, one molecule can act as donor to the Mg atom of another *via* the keto C=O function. As a result of the operation of these donor–acceptor forces, chlorophyll in nonpolar solvents such as benzene or carbon tetrachloride forms dimers, (Chl_2), and, in aliphatic hydrocarbon solvents, oligomers, $(Chl_2)_n$.[6-10]

In vivo studies show that chlorophyll in the plant is organized into large photosynthetic units[12] consisting of several hundred chlorophyll molecules. Most of the Chl *a* in the unit is not photoreactive and appears to serve as an antenna for collecting light quanta. Antenna chlorophyll in the plant absorbs light in the red region of the visible spectrum near 680 nm. Thus, the absorption maximum of antenna Chl *a* is red-shifted relative to that of Chl *a* solutions in polar solvents, which generally have their red absorption maxima at 662–665 nm.

We have advanced the hypothesis[13-15] that antenna chlorophyll in green plants is very similar to, if not identical with, the Chl *a* oligomers, $(Chl_2)_n$, present in concentrated Chl *a* solutions in aliphatic hydrocarbon solvents. In these oligomers, the chlorophyll molecules are held together by keto C=O···Mg interactions, and the spectral properties are considered to be largely the consequences of the particular spatial arrangement of the chlorophyll molecules relative to each other.

Our primary concern in this study, therefore, is to obtain information about the structure of the chlorophyll dimers from which chlorophyll oligomers *in vitro* and presumably antenna chlorophyll *in vivo* are constituted.

From infrared, visible, ^1H, and ^{13}C nmr spectroscopic studies it has been established that in dry nonpolar solvents like carbon tetrachloride and benzene, Chl *a* occurs as a dimer over a very large concentration range.[6,7] The equilibrium $2Chl \rightarrow Chl_2$ in these solvents is displaced very far to the right, with an equilibrium constant probably larger than 10^6. The concentration of monomeric chlorophyll in these solutions must be very small indeed. Although ^1H nmr has been successfully used[3,5] to establish the presence of (Chl_2) dimers in CCl_4 and benzene and to make some deductions about the geometry of the dimer, further structural information is highly desirable for the interpretation of visible absorption spectra. As it has not as yet been possible to apply X-ray diffraction methods to aggregated chlorophyll structures, we have explored the utility of ^1H nmr in conjunction with shift reagents, with structural information as the objective.

In this communication, we describe ^1H nmr lanthanide shift reagent studies designed to elicit structural information about chlorophyll dimers. Visible spectroscopy and computer deconvolution of Chl *a* solution

(1) This work was performed under the auspices of the U. S. Atomic Energy Commission.
(2) E. I. Rabinowitch, "Photosynthesis," Vol. II, Part 1, Interscience, New York, N. Y., 1951, p 1142.
(3) J. J. Katz, R. C. Dougherty, and L. J. Boucher, in "The Chlorophylls," L. P. Vernon and G. R. Seely, Ed., Academic Press, New York, N. Y., 1966, Chapter 7, pp 185–251.
(4) J. J. Katz, G. L. Closs, F. C. Pennington, M. R. Thomas, and H. H. Strain, *J. Amer. Chem. Soc.*, **85**, 3801 (1963).
(5) G. L. Closs, J. J. Katz, F. C. Pennington, M. R. Thomas, and H. H. Strain, *J. Amer. Chem. Soc.*, **85**, 3809 (1963).
(6) J. J. Katz and T. R. Janson, *Ann. N. Y. Acad. Sci.*, **206**, 579 (1973).
(7) J. J. Katz, T. R. Janson, A. G. Kostka, R. A. Uphaus, and G. L. Closs, *J. Amer. Chem. Soc.*, **94**, 2883 (1972).
(8) J. J. Katz, K. Ballschmiter, M. Garcia-Morin, H. H. Strain, and R. A. Uphaus, *Proc. Nat. Acad. Sci. U. S.*, **60**, 100 (1968).
(9) J. R. Norris, M. E. Druyan, and J. J. Katz, *J. Amer. Chem. Soc.*, **95**, 1680 (1973).
(10) K. Ballschmiter, K. Truesdell, and J. J. Katz, *Biochim. Biophys. Acta*, **184**, 604 (1969).
(11) J. J. Katz, *Develop. Appl. Spectrosc.*, **6**, 201 (1968).
(12) E. Rabinowitch and Govindjee, "Photosynthesis," Wiley, New York, N. Y., 1969, p 69.
(13) J. J. Katz and J. R. Norris, *Curr. Top. Bioenerg.*, **5**, 41 (1973).
(14) J. J. Katz, *Naturwissenschaften*, **60**, 132 (1973).
(15) K. Ballschmiter and J. J. Katz, *Nature (London)*, **220**, 1231 (1968).

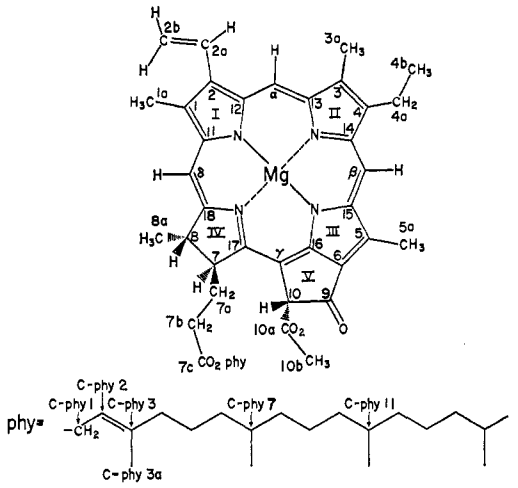

Figure 1. The structure and numbering system for chlorophyll *a*. Methylpheophorbide *a* has two hydrogens instead of Mg and CH_3 in place of phytyl at 7c.

spectra with added shift reagents provided further insights into the structure of Chl *a* dimers. In contrast to the usual shift reagent studies of molecules, in which the structural information is deduced from the determination of the bound chemical shifts (Δ_B), in this study we use shift reagents as a tool complementary to the X-ray diffraction methods. We are trying to obtain the structural information about the aggregation of Chl *a* in solution, so we have first completed a related ^1H nmr study of methylpheophorbide *a* and methylbacteriopheophorbide *a*, Mg-free derivatives of chlorophyll. These studies were undertaken as a desirable preliminary to provide experience in simpler systems on the consequences of the binding of shift reagents to such large molecules as chlorophyll.

The information we obtained from the pheophorbide work, especially that relating to the structure of the substrate–shift reagent complex and to the binding of europium to the keto C=O group on the ring V, considerably facilitates an approach to the Chl *a* dimer problem. As it turns out, the π–π interaction of the two macrocycles in the Chl *a* dimer is of comparable strength to that of the lanthanide-induced chemical shifts. Thus, with the knowledge of the binding sites of Eu(III) to the Chl *a* macrocycle, we can interpret the structural changes in the Chl *a* dimer induced by the binding of the shift reagent. Furthermore, the complementary study of the visible absorption spectra of the same Chl *a*–Eu(fod)$_3$ solutions we describe here provides us with additional information about the dimer structure in solution.

Experimental Section

Preparation of Compounds. Methylpheophorbide *a* was prepared and purified by the method of Strain.[16] Before use it was extensively dried by pumping *in vacuo* and stored in a vacuum desiccator. Methylbacteriopheophorbide *a* was prepared by B. Cope of the ANL Chemistry Division by standard procedures and was throughly dried before use. Chlorophyll *a* and [^2H]chlorophyll *a* were prepared by B. Cope, were rechromatographed on a sugar column, and thoroughly dried before use.[17]

Lanthanide Shift Reagents. Commercial grade reagents were used without further purification except for thorough drying *in vacuo*. Every series of shift reagent experiments was calibrated for "inactive" shift reagent concentration (see below).

Solvents. All solvents were dried, distilled, and stored over appropriate molecular sieves.

^1H Nmr Spectra. Samples were prepared by dissolving 0.5–15 mg of Chl *a* or the methylpheophorbide in 0.5 ml of the appropriate solvent; 5 μl of hexamethyldisiloxane (HMS) was added and used to provide the FT homonuclear lock. Only fresh, degassed samples were used, usually within hours of preparation. ^1H nmr spectra were recorded with a Varian HA-100 spectrometer modified for FT operation. All chemical shifts are given in δ, ppm, downfield from HMS. Probe temperature was measured by methanol temperature calibration samples.

Visible Absorption Spectra. Samples for visible spectroscopy were prepared with utmost care to avoid contamination by adventitious water vapor. Drybox techniques were used throughout in conjunction with vacuum line techniques for degassing and drying solutions. Chl *a* runs with Eu(fod)$_3$ in benzene were performed in 5-mm cells, and runs in CCl_4 were performed in 2-mm cells. Visible spectra were recorded on a modified Cary 14 spectrometer, and digitized data were inserted directly into the Chemistry Division Sigma 5 XDS computer.

Computations. Least-square analyses of the experimental data were performed by standard library routines on the Sigma 5 XDS computer of the Chemistry Division. LISHIFT calculations and structure plotting were carried out on the IBM 360-195 computer of the Applied Mathematics Division (AMD) of the Argonne National Laboratory. The LISHIFT program used was the modified version of LISHIFT program kindly furnished by Dr. G. Slomp of Upjohn Co., Kalamazoo, Mich. Molecular structure plots were produced by the Oak Ridge Thermal Elipsoid Plot Program (ORTEP).[18] The AMD Variable Metric Minimization library program for spectra deconvolution was modified and adapted to use on our Sigma 5 by A. Zielen of the ANL Chemistry Division.

Results and Discussion

Pheophorbides and Shift Reagents. Lanthanide shift reagents have been applied to numerous structural studies since their recent discovery by Hinckley.[19,20] However, there have not been many examples of shift reagent studies of large and complex molecules.[21–24] The large size of porphyrin-type molecules such as methylpheophorbide *a* requires the use of the most powerful shift reagents, and even then shifts of the more distant protons (>12 Å) are quite small, and thus the experimental errors can be large. Furthermore, the use of shift reagents such as Eu(fod)$_3$ and Pr(fod)$_3$ that have large binding constants precludes accurate determination of equilibrium constants and the stoichiometry of the substrate–lanthanide complex. Nevertheless, as we show here, valuable structural information can still be obtained from such studies.

The most suitable method for accurate determination of the bound chemical shifts Δ_B of the substrate–lanthanide complex is the procedure of Armitage, *et al.*[25] There is no simple way to extract Δ_B from a single plot of δ *vs.* $[L]_0/[S]_0$, where δ is the chemical shift of the proton under study, and $[L]_0$ and $[S]_0$ are the concentrations of lanthanide shift reagent and sub-

(16) F. C. Pennington, H. H. Strain, W. A. Svec, and J. J. Katz, *J. Amer. Chem. Soc.*, **86**, 1418 (1964).
(17) H. H. Strain and W. A. Svec in ref 3, pp 21–61.
(18) C. K. Johnson, "ORTEP: A FORTRAN Thermal Elipsoid Plot Program for Crystal Structure Illustrations," ORNL Report, Oak Ridge, Tenn., 1965, 3794.
(19) C. C. Hinckley, *J. Amer. Chem. Soc.*, **91**, 5160 (1969).
(20) For a recent review, see J. Reuben, *Progr. Nucl. Magn. Resonance*, **9**, 1–65 (1973).
(21) A. R. Katritzky and A. Smith, *Brit. Polym. J.*, 4, 199 (1972).
(22) H. Kjosen and S. Liaaen-Jensen, *Acta Chem. Scand.*, **26**, 218 (1972).
(23) L. D. Hall, J. F. Manville, and N. S. Bhacca, *Can. J. Chem.*, 47, 1 (1969).
(24) N. S. Angerman, S. S. Danyluk, and T. A. Victor, *J. Amer. Chem. Soc.*, **94**, 7137 (1972).
(25) I. Armitage, G. Dunsmore, L. D. Hall, and A. G. Marshall, *Can. J. Chem.*, **56**, 2114 (1972).

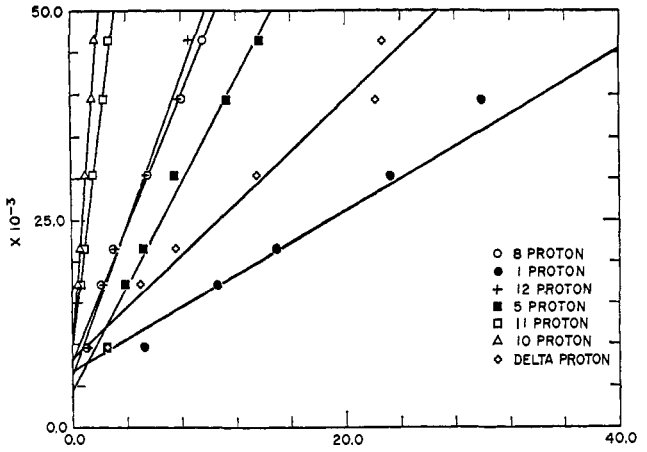

Figure 2. CalComp plot of least-squares fit of methylpheophorbide and Eu(fod)$_3$ (7.13×10^{-3} *M*) titration. $1/\delta$ is plotted along the abscissa and methylpheophorbide *a* concentration is plotted along the ordinate. Note on labeling: Label 8 proton is a label for 8a methyl group protons, 1 proton for 1a methyl group proton, 5 proton for 5a methyl group proton, 11 proton for a methyl group proton in 10b position, and 12 proton for a methyl group in place of phytol at 7c.

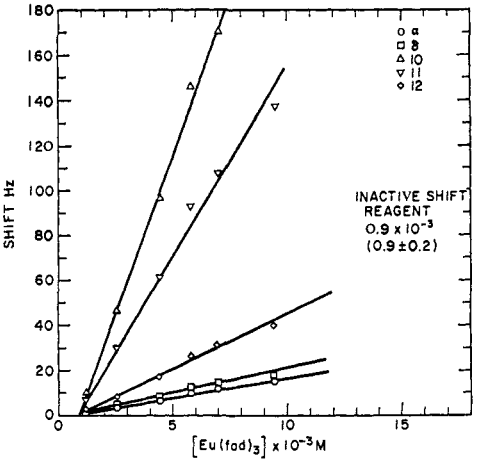

Figure 3. Determination of the inactive shift reagent concentration. Data for methylbacteriopheophorbide and Eu(fod)$_3$ experiments. Methylbacteriopheophorbide concentration 1.62×10^{-2} *M*.

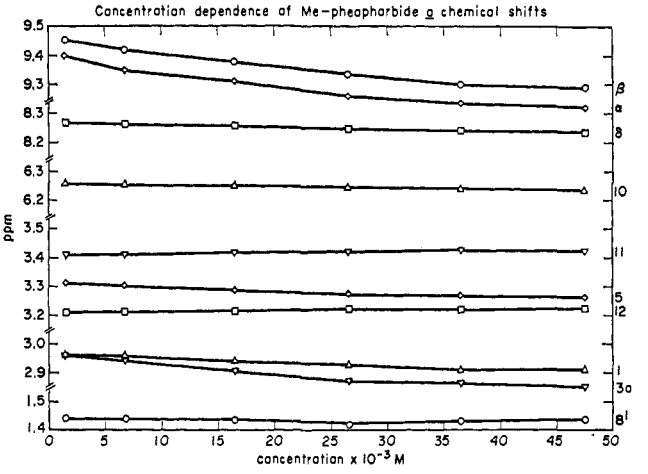

Figure 4. Concentration dependence of methylpheophorbide *a* chemical shifts in C_6D_6 at room temperature in the range of 1–46 $\times 10^{-3}$ *M*.

strate, respectively. Furthermore, $[L]_0$, the lanthanide shift reagent concentration, must remain constant in an experiment to avoid complications due to changes in the bulk susceptibility of the solution. Thus, experiments were performed by varying $[S]_0$, holding $[L]_0$ constant, and a plot was made of $1/\delta$ *vs.* $[S]_0$. This procedure gives a straight line, where the slope is $[L]_0\Delta_B$, and the *y* intercept is $-[(1/K_B) + [L]_0]$, K_B being the binding constant.[25] This method is valid when $[L]_0/[S]_0 < 1$, so that all experiments were carried out in that concentration range.

The determination of the bound shift Δ_B for Eu(fod)$_3$ and methylpheophorbide *a* and methylbacteriopheophorbide *a* was carried out by this procedure. Figure 2 illustrates the $1/\delta$ *vs.* $[S]_0$ plots obtained by the least-squares treatment of the experimental data for methylpheophorbide *a*. The "inactive" shift reagent concentration was determined for several runs (Figure 3). The inactive shift reagent was found to be $(0.9 \pm 0.2) \times 10^{-3}$ *M* in methylbacteriopheophorbide *a* runs and 0.8×10^{-3} *M* in methylpheophorbide *a* runs in C_6D_6. Small residual amounts of water vapor, as well as other possible contaminants present in solutions of chlorophyll and its derivatives, may bind preferentially to the shift reagent and reduce the effective shift reagent concentration. Furthermore, commercial shift reagents contain impurities that are difficult to remove by crystallization procedures. Thus, it is useful to determine the actual shift reagent concentration by measuring the "inactive" shift reagent concentration in all the systems studied. This quantity can be determined by plotting shift reagent concentration $[L]_0$ *vs.* δ shift of a proton(s) of the substrate in question.[25] The substrate concentration is held constant while shift concentration is varied. If no "inactive" shift reagent is present, *i.e.*, if there are no losses to impurities in solution or in the shift reagent itself, the line should pass through the origin. The *x* intercept (Figure 3) gives a value of the "inactive" shift reagent concentration. To obtain an exact Δ_B, a correction for the stacking of pheophorbide macrocycles in solutions, which causes a small upfield shift (Figure 4), was also made. This form of π–π aggregation, which must be clearly differentiated from the keto C=O···Mg aggregation that we are concerned with here, occurs only with methylpheophorbide *a* and (surprisingly) is not observed for methylbacteriopheophorbide *a* in the same concentration range.

The structure correlations of the Eu(fod)$_3$ induced shifts were determined through a least-squares fit using the LISHIFT program (Figure 5). While an approximate correlation of the induced paramagnetic shifts based on a $1/r^3$ dependence, where *r* is the distance between Eu and the proton in question, is generally found, small deviations from the $1/r^3$ dependency are usually explained by possible contact shift contribution and/or the failure to consider the angular dependence portion of the pseudocontact relationship.[26,27] In our case, a substantial distance of the closest proton to Eu (≥ 3 Å) precludes any important contact shift contribution.

It is not surprising that while even the most naive structure correlations yield approximate $1/r^3$ depen-

(26) E. Caple, D. K. Harris, and S. C. Kuo, *J. Org. Chem.*, **38**, 381 (1973).

(27) R. Von Amman and R. D. Fischer, *Angew. Chem., Int. Ed. Engl.*, 11, 675 (1972).

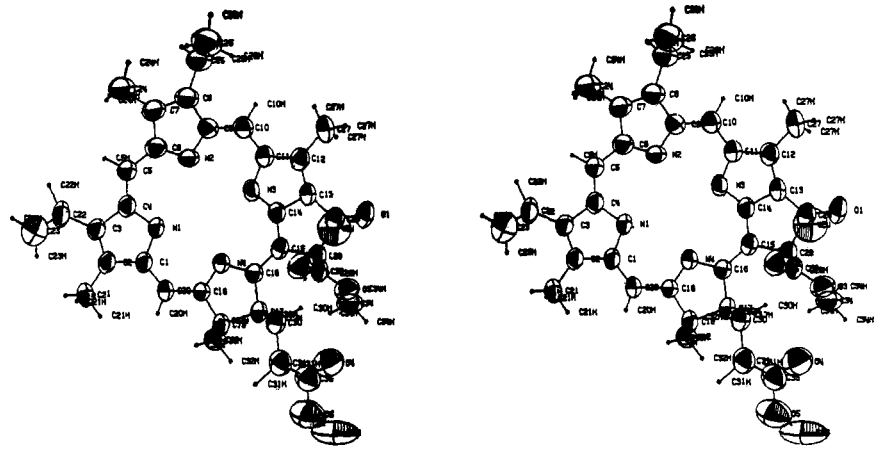

Figure 5. ORTEP stereo drawing of methylpheophorbide *a* and Eu as determined by the LISHIFT program. R = 0.087. Eu is complexed both to C=O of ring V (01) and ester C=O at position 10a (03). NH protons have been omitted from the drawing. Eu can be found as a larger round ellipsoid behind the ring V C=O carbon atom (C28–O1).

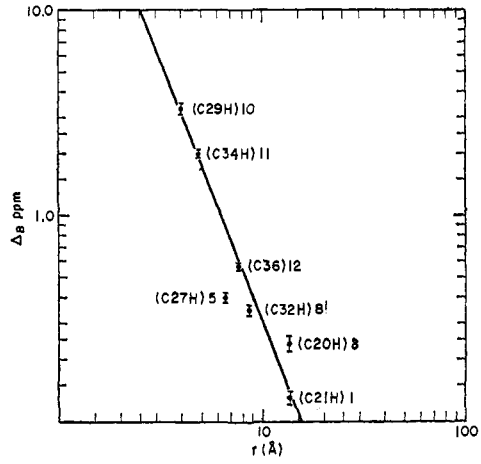

Figure 6. Log-log plot of observed Δ_B *vs. r;* the slope is approximately −3. Eu atom is positioned 2.5 Å from C=O oxygen shifted in plane of macrocycle 2 Å from Eu–O–C ∢180° position.

Table I. Methylpheophorbide *a* and Eu(fod)$_3$

Proton	Obsd shift	Calcd shift
C21H(1aH)[a]	0.13	0.10
C21H(1aH)	0.13	0.10
C21H(1aH)	0.13	0.10
C32H(8aH)	0.35	0.20
C32H(8aH)	0.35	0.20
C32H(8aH)	0.35	0.20
C20H(δH)	0.24	0.51
C29H(10H)	3.34	3.33
C27H(5aH)	0.40	0.40
C27H(5aH)	0.40	0.40
C27H(5aH)	0.40	0.40
C34H(10bH)	2.00	2.00
C34H(10bH)	2.00	2.00
C34H(10bH)	2.00	2.00
R factor = 0.08		

[a] Proton labeling as in Figure 1.

dence, it is necessary to use all the angular factors (LISHIFT program) to obtain a realistic structure of the substrate–shift reagent complex. For example, placing Eu in the plane of the methylpheophorbide *a* macrocycle 2.5 Å from the keto C=O···oxygen, and shifted in plane 2 Å from the Eu–O–C ∢ 180° position, yields a reasonable $1/r^3$ correlation (Figure 6). We have tried several similar structure correlations. In general, an approximate $1/r^3$ correlation was obtained in every case for several positions of Eu placed about 2–3 Å in plane with macrocycles with Eu–O–C angles of 180° or less.[28] However, the final structure of the methylpheophorbide *a*–Eu complex is somewhat different when the LISHIFT program was used (Figure 5, Table I) with all the angular factors. In particular, the final structure of methylpheophorbide *a*–Eu complex shows Eu behind the plane of macrocycle coordinated not only to the ring V keto C=O function but also to the ester C=O in the propionic acid group at position 11. The need to consider all the pseudocontact angular terms illustrates an effect that we feel will be observed in most large molecules. Small induced shifts (Δ_B) and the large number of protons that have to be considered require the use of a sophisticated iterative least-squares program to calculate adequately the shifts and to give a reasonable structural fit. There is an ongoing debate as to the justification and accuracy of the pseudocontact angular terms and their use in the structural correlations using LIS data.[20,27] While for our purposes it is sufficient to show that the keto C=O group of the ring V is the binding site of the shift reagent, it may be a useful exercise to attempt a structural correlation with our LIS data.

The induced paramagnetic shift correlations using the LISHIFT program in the case of methylbacteriopheophorbide *a* (R = 0.20) are only fair (Table II). This was expected because no crystal structure is known for methylbacteriopheophorbide *a*, and methylpheophorbide *a* crystal data were therefore used for methylbacteriopheophorbide *a*.[29]

It is interesting to compare the ^{1}H nmr results for the two pheophorbides. Methylbacteriopheophorbide *a* interacts more strongly with the shift reagent, and it is bound for the most part only through its ring V keto C=O group. Methylpheophorbide *a* is bound less strongly, and Eu is bound not only by the keto C=O function of ring V, but by the ester C=O in the propionic acid group at position 11. The saturation of

(28) We acknowledge with thanks the contribution of Dr. J. Williams of ANL Chemistry Division in this particular effort.

(29) M. S. Fischer, D. H. Templeton, A. Zalkin, and M. Calvin, *J. Amer. Chem. Soc.*, **93**, 2622 (1971).

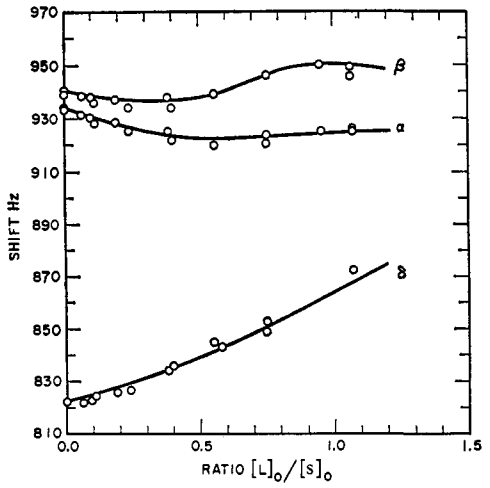

Figure 7. Chl *a* $[S]_0$ and Eu(fod)$_3$ $[L]_0$ in C_6D_6. Shifts of low-field lines of methine protons are illustrated.

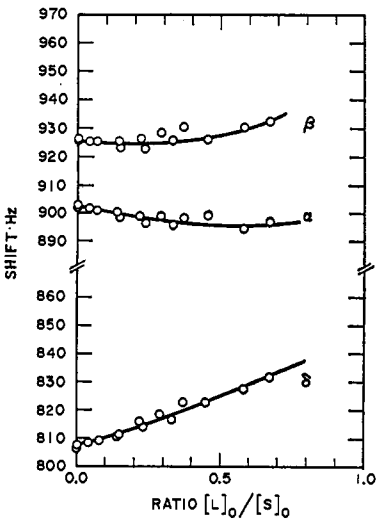

Figure 8. Chl *a* $[S]_0$ and Eu(fod)$_3$ $[L]_0$ in CCl_4. Shifts of methine protons are illustrated.

Table II. Methylbacteriopheophorbide and Eu(fod)$_3$

Proton	Obsd shift	Calcd shift
C21H(1aH)[a]	0.80	0.70
C21H(1aH)	0.80	0.70
C21H(1aH)	0.80	0.70
C32H(8aH)	2.52	2.46
C32H(8aH)	2.52	2.46
C32H(8aH)	2.52	2.46
C20H(δH)	0.96	2.31
C5H(αH)	0.71	0.40
C10H(βH)	0.36	−0.50
C29H(10H)	12.85	15.04
C27H(5aH)	0.84	0.80
C27H(5aH)	0.84	0.80
C27H(5aH)	0.84	0.80
C34H(10bH)	8.00	6.10
C34H(10bH)	8.00	6.10
C34H(10bH)	8.00	6.10
R factor = 0.22		

[a] Proton labeling as in Figure 1.

double bond in ring II of methylbacteriopheophorbide *a* relieves some strain in the exocyclic ring V, and generally makes the whole molecule less strained and more flexible along its saturated backbone consisting of rings II and IV. Thus, it is not surprising that the keto C=O group of ring V plays a more prominent role in coordination with Eu as compared to the more strained methylpheophorbide *a* case. There appears to be no observable binding by magnetic resonance criteria at the carbonyl position 2 in methylbacteriopheophorbide.

The structural correlations derived from the shift reagent studies are compatible with and support the published X-ray diffraction data for methylpheophorbide *a*.[29] Our results also indicate that methylbacteriopheophorbide *a* and methylpheophorbide *a* are structurally quite similar. But, as we have pointed out earlier, the structure correlations using lanthanide shift reagents cannot successfully compete in precision with X-ray diffraction work. Only first-order structural information is obtainable in LIS studies in the case of these large and complex molecules. However, we can now approach the applications of the nmr technique to (Chl_2) with considerably more confidence.

Chlorophyll and Shift Reagents. Chl *a* solutions in carefully purified carbon tetrachloride and benzene are known from direct molecular weight measurements to contain for the most part chlorophyll dimers.[10] The ^1H nmr spectra of (Chl_2) in these solutions are only partially resolved, on the one hand, because of the long correlation times of the dimer, and, on the other hand, because of ring current effects on the chemical shifts of protons by adjacent chlorophyll rings. Chl *a* in solutions in methanol and tetrahydrofuran is monomeric, $Chl \cdot L_1$, but shift reagents cannot be used in the presence of such nucleophiles because of competition for coordination to the rare earth ion. However, in spite of the inability to obtain totally resolved ^1H nmr spectra for the dimers, valuable information can still be obtained by studying Chl *a* dimer spectra in the presence of shift reagents.

The observed shifts on the addition of shift reagents in benzene and carbon tetrachloride solutions are very small, and thus no attempt was made to determine the bound chemical shift Δ_B. However, observations of considerable interest can be made when plots of δ *vs.* $[L]_0/[S]_0$ for (Chl_2) are made (see Figures 7 and 8). As the amount of lanthanide shift reagent is increased the normal behavior that we have observed with the pheophorbides is not observed with the (Chl_2). Rather, the chemical shifts of some protons in the (Chl_2) dimer at first move to higher field, and only then shift to the lower field normally expected from the action of the shift reagent. The "normal" response only becomes apparent when the $[L]_0/[S]_0$ ratio becomes larger than 0.5 for benzene solutions, and about 0.3 for CCl_4 solutions. Furthermore, it is important to point out this anomalous behavior does not hold for all protons: for example, the δ protons exhibit quite normal behavior and move to lower field as soon as shift reagent is introduced. The methine α and β protons, however, show this initial shift to higher fields in the chemical shift *vs.* $[L]_0/[S]_0$ plots, indicating an increase of macrocycle overlap in those regions of the molecule, which must result from the shift reagent addition. The obvious rationalization for this unusual state of affairs is that there are a number of different dimer conformations present in the dimer solutions, and that the relative populations of conformers of the dimer are affected by the addition of the shift reagent. We see only single

resonances in ^1H nmr spectra, indicating that mobile equilibrium between the conformers is fast on the nmr time scale. The fact that it appears that the minima occur at a $[L]_0/[S]_0$ ratio of 0.5, or less than 1, is consistent with the view that we are dealing only with dimeric chlorophyll species in these solutions. Because dimer formation is assumed to involve the 9-keto C=O group of one chlorophyll and the central Mg atom of another chlorophyll molecule, there is only one free 9-keto group in the dimer. That such is the case is indicated by the chlorophyll titration studies of Closs, *et al.*[5] In the case of a 1:1 complex, *e.g.*, (Chl a_2)–Eu, there should be a maximum lanthanide induced shift at a ratio of 0.5. However, a small binding constant would shift the maximum to a higher ratio, as in fact is observed. Furthermore, the (Chl_2) dimer ^1H nmr spectrum in benzene or carbon tetrachloride has much better resolved resonances than a spectrum of chlorophyll oligomers, $(Chl_2)_n$, such as are present in chlorophyll solutions in *n*-octane.[6] While $(Chl_2)_n$ oligomer spectra in *n*-octane show an increase in the number of resolved spectral lines on heating, this is not the case when chlorophyll dimers are heated in toluene. There is essentially no change in number or chemical shift of resolved resonances in (Chl_2) in toluene-d_8 on heating up to 90°. This was expected since at room temperature we are essentially at the fast exchange limit. Variable temperature study (10–90°) also failed to yield any new details of the chlorophyll–chlorophyll interactions primarily due to the extensive broadening of the few resolved proton resonances even at +10°. Thus, we can conclude with some confidence that the chlorophyll species we are dealing with in benzene and carbon tetrachloride solution is chlorophyll *a* dimer. To gain more insight about the solvent dependence of shift reagent behavior with Chl *a*, an attempt was made to monitor the single ^1H resonance of the $Eu(fod)_3$. For this purpose [^2H]Chl *a* was used. However, only a small solvent dependence of the chemical shift can be seen in such an experiment, and no definite clue as to the structural difference between (Chl_2) in benzene and carbon tetrachloride solutions could be obtained.

The tentative conclusions that emerge from the ^1H nmr work are that the structures of Chl *a* dimer in dry carbon tetrachloride and benzene are similar but are solvent dependent in detail. Two important effects influence the chemical shifts in the presence of the shift reagent in Chl *a* solutions. The π–π interactions of the macrocycles and the shift reagent cause shifts in the opposite direction. A reasonable explanation is that a more overlapping conformer of the Chl *a* dimer becomes more favored as the $Eu(fod)_3$ concentration is increased. We now turn to the visible spectroscopy to seek confirmation of these interpretations. The utility of the electronic transition spectra is considerably facilitated by computer deconvolution of the envelopes of the visible spectra, and the results from visible absorption spectroscopy are consistent and reinforce the structural conclusions inferred from the ^1H nmr shift reagent studies on (Chl_2).

Computer Deconvolution of Visible Spectra. Antenna chlorophyll in green plants appears to be structurally very similar to chlorophyll oligomers $(Chl_2)_n$ *in vitro*. This conclusion is based on numerous studies of visible absorption spectra of chlorophyll solutions.[29–35] Antenna chlorophyll in plants has its absorption maximum in the red near 680 nm. Computer deconvolution of the visible absorption spectra of *in situ* antenna chlorophyll and of chlorophyll oligomers in nonpolar solvents reveals a high degree of similarity between the Gaussian components of the two red envelopes.[35]

For curve resolution a program written by Applied Mathematics Division of Argonne National Laboratory was modified and adapted for Chemistry Division Sigma computer. The program uses a variable metric minimization of Davidon.[36] This least-squares program has the outstanding feature of being able to converge even in the most difficult nonlinear problems.

The envelope of the visible spectrum can be resolved into components by the least-squares fit of a specified number of Gaussian or Lorentzian components, or a mixture of the two. In this work, we have chosen to use pure Gaussian line shapes because monomeric chlorophyll *a* solutions in polar solvents have a red envelope very nearly truly Gaussian. Furthermore, statistical theory tells us that the shape of the line is determined by the distribution of the instantaneous fields over a variety of atoms. The effect of other atoms on a given atom can be approximated by a static rather than sudden impact. The line shape is due to the fact that different atoms are exposed to different fields, or equivalently, that the field is only quasistatic, and varies slowly in time. If a given atom interacts with a large number of neighbors, so that the total field is compounded from a large number of small fields, the distribution of resultant fields should presumably be approximately Gaussian, for the Gaussian situation is a quite general consequence of the statistics of aggregates of a large number of objects.[37]

The above criteria for Gaussian line shape should be fulfilled in chlorophyll aggregates.

The spectra of chlorophyll *a* in dilute solutions in carbon tetrachloride show a distinct shoulder but concentrated solutions have a smooth and quite structureless red envelope. Thus, while there is little difficulty in realizing unique deconvolutions for the spectra of dilute solutions, the deconvolution of the concentrated solutions gives several equally good fits. However, a self-consistent deconvolution over the entire concentration range (10^{-6}–10^{-1}) has been achieved.[35] The concentration range used in this work is in the middle range (10^{-3} and 10^{-2} *M*) and the red envelopes show moderate shoulders of the red absorption maxima. Furthermore, a self-consistent deconvolution was possible which in turn was consistent with the previous deconvolution work mentioned above.[35] The visible absorption envelope between 740 and 655 nm was deconvoluted into three (3) Gaussian components: 666 ± 2, 680 ± 2, and 695 nm. The component at 695 is

(30) C. N. Cederstrand, E. Rabinowitch, and Govindjee, *Biochim. Biophys. Acta*, **126**, 1 (1966).
(31) C. S. French, *Proc. Nat. Acad. Sci. U. S.*, **68**, 2893 (1971).
(32) C. S. French and L. K. Praeger in "Progress in Photosynthesis," Vol. II, H. Metzner, Ed., Tubigen, 1969, p 555.
(33) C. S. French, J. S. Brown, and M. C. Laurence, *Plant Physiol.*, **49**, 421 (1972).
(34) B. A. Gulyayev and F. F. Litvin, *Biophysics (USSR)*, **12**, 970 (1967).
(35) T. M. Cotton, A. D. Trifunac, K. Ballschmitter, and J. J. Katz, submitted for publication in *Biochim. Biophys. Acta*.
(36) W. C. Davidon, "Variable Metric Method of Minimization," ANL Report 5990, Argonne, Ill., 1959.
(37) J. H. Van Vleck, *Nuovo Cimento, Suppl.*, **6**, 993 (1956).

needed to reproduce tailing off toward 740 nm. The important feature of deconvolution of both benzene and carbon tetrachloride solutions of chlorophyll *a* with $Eu(fod)_3$ is the variation of the ratio of 666 and 680 peaks with varying $Eu(fod)_3$ concentration as illustrated in Figure 9.

Addition of $Eu(fod)_3$ causes the growth of the 680-nm component and overall peak shift to red. The 680-nm component, which is initially very small, becomes a dominant component when the $[Eu(fod)_3]/[Chl\ a]$ ratio becomes greater than 0.5–0.7 depending on a solvent. It was previously suggested that the 680-nm component is related to macrocycle overlap. Besides the nmr results tell us that there is an increase in macrocycle overlap when $Eu(fod)_3$ is added. The deconvolution of the spectra in two solvents without any $Eu(fod)_3$ present indicates that there are some differences in the properties of conformers, in the two solvents. In benzene there is more 680-nm component initially present and it takes more shift reagent to produce a population change. This is in agreement with nmr data which show that population changes of the two (or more) conformers show solvent dependence. The nmr and deconvolution results indicate that there is more ordering in benzene solutions so that proportionally more shift reagent is needed to cause population change of chlorophyll conformers in benzene solution.

Summary

The LIS studies of chlorophyll *a* in solutions of dry benzene and carbon tetrachloride indicate that there is a change of conformer populations under the influence of the shift reagent. It is important to point out that by "conformer population" we do not imply any strict one-to-one correspondence between the intensity of the bands obtained by the deconvolution of the envelopes of the visible spectra, and the population of the various conformations of Chl *a* dimer. However, as the following discussion will attempt to show, the two effects must be related. It is well known that the 666-nm (monomer) band is intrinsic to the macromolecular system, and the 680-nm band can be properly called an interaction band. The relative importance of these two bands in the Chl *a* dimer spectrum is related to the prevalent geometry or conformer population of the dimer, since the band intensity is a consequence of the geometric relationship of transition dipole moments. The observed increase in the macrocycle overlap would be reflected in the increase of the interaction band contribution to the spectral envelope. The interaction of the transition dipole moments in trimers and oligomers of Chl *a* might be expected to result in further interaction bands, but these in fact are not observed. It could very well be that such higher order interactions are either too small to be observed, or cannot be separated from the larger dimer contributions.

This view is substantiated by the deconvolution of the envelopes of the visible spectra of the same solution. The two results allow us to draw some tentative conclusions regarding the conformation of Chl *a* dimer in the two solvents. Chlorophyll *a* dimer in these solvents may be regarded as existing in at least two conformations that differ by the extent of macrocycle overlap and/or the angle between the plane of two macrocycles. The relative populations of the two (or more) conformers change when shift reagent is added, indicating that the equilibrium is shifted toward the more overlapping conformer. This may be due to steric requirements of shift reagents binding to the free ring V keto group. In its general features the suggested Chl *a* dimer model of Closs, *et al.*,[5] and of Houssier and Sauer[38] is in agreement with our data. However, we must indicate some important modifications required of that model. The Chl *a* dimer is a mobile structure and not a rigid one, as might be inferred from the model of Houssier and Sauer.[38] The nmr data indicate that the probable (average) structure of Chl *a* dimers is best represented by two porphyrin rings inclined with respect to each other, with the keto C=O group of one Chl *a* molecule interacting with the Mg of the other. However, the nmr data require equivalence of the two molecules of Chl *a* that make up the dimer. The relatively sharp line width shows that the mean lifetime of the associated species must be short.[5] In particular, this process would seem to be faster than the rather mobile equilibrium in the Chl *a*–Eu complex, as nonequivalence of protons is not seen. The Eu interacts with the keto C=O group and complexation thus favors the dimer conformation in which the two Chl *a* molecules become more overlapped in some regions. The reasonable structure of the dimer would be one in which two macrocycles are inclined with respect to each other in such a way as to require minimal motion to complete the switch of keto $C{=}O^1\cdots Mg^2 \rightleftharpoons C{=}O^2\cdots Mg^1$ interactions. The steric requirements of $Eu(fod)_3$ binding would require more space around the keto C=O group, thus increasing the twist angle by causing rotation of the macrocycle planes with respect to each other. These considerations are consistent with the results of deconvolution of visible spectra of Chl *a* oligomers, which indicate an increased population of more overlapping conformers. The model we suggest here is consistent with present and previous data, but a final detailed dimer structure still eludes us.

The population of conformers is solvent dependent. These and previous[13–15] studies allow us to extrapolate

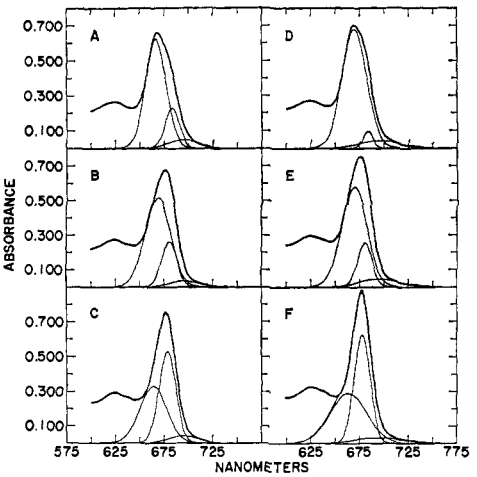

Figure 9. Computer deconvolution of the envelopes of visible spectra (thick lines) of Chl *a* and $Eu(fod)_3$ in C_6H_6 and CCl_4 solutions. Figures A, B, and C represent Chl *a* (2.37×10^{-5} *M*) in benzene and 0, 1.33×10^{-5}, and 2.23×10^{-5} *M* $Eu(fod)_3$, respectively. Figures D, E, F represent Chl *a* (6.2×10^{-5} *M*) in CCl_4 and 0, 1.29×10^{-5}, and 6.45×10^{-5} *M* $Eu(fod)_3$, respectively.

(38) C. Houssier and K. Sauer, *J. Amer. Chem. Soc.*, **92**, 779 (1970).

to the *in vivo* situation of antenna chlorophyll, and to suggest that antenna chlorophyll consists of units of chlorophyll dimers in which the macrocycles show overlap between the individual chlorophyll molecules. The presence of extraneous nucleophiles, concentration, and/or the nature of the environment determine the relative populations of the conformers.

The extent of macrocycle overlap and the ease of population change of conformers in antenna chlorophyll in the plant should have tremendous influence on the performance of bulk chlorophyll in its light-gathering role in photosynthesis. The great similarity between the deconvoluted red bands of antenna chlorophyll in the plant and that of a concentrated Chl *a* solution in aliphatic hydrocarbon solvents, which contain chlorophyll *a* oligomers with molecular weight of 20,000, provides a basis for the identification of *in vivo* antenna chlorophyll in green plants with $(Chl_2)_n$ dimers. The problems involved in obtaining structural information on antenna chlorophyll *in situ* and chlorophyll oligomer *in vitro* are formidable. The indications that the spectral properties of the oligomer, and inferentially of antenna chlorophyll, are largely determined by the Chl–Chl interaction in the dimer unit make the structural conclusions derived from the joint application of ^1H nmr and visible absorption spectroscopy particularly relevant to the *in vivo* situation.

Acknowledgments. We thank Dr. J. Williams of the Chemistry Division of Argonne National Laboratory for his generous assistance in our early efforts in induced paramagnetic shift correlations, and for furnishing the ORTEP plotting program. We thank Dr. G. Slomp of Upjohn Company of Kalamazoo, Mich., for furnishing LISHIFT program. We also wish to acknowledge the efforts of Mr. A. Zielen of the Chemistry Division of ANL in adapting and modifying the computer program used in the deconvolution of the visible spectra.

Communications to the Editor

Orbital Isomerism as a Controlling Factor in Chemical Reactivity[1]

Sir:

Pericyclic reactions[2] have mostly been interpreted either in terms of correlations of states[3] or orbitals[2,4] between reactants and products, based on the assumption that some element of symmetry is retained throughout the reaction, or in terms of the idea first put forward by Evans[5] that the transition states of pericyclic reactions are isoconjugate with cyclic π systems and so can likewise be specifically stabilized or destabilized relative to open chain analogs, *i.e.*, aromatic or antiaromatic.[6] Here we wish to put forward a more general approach that represents in effect a synthesis of the earlier ones.

Consider a pericyclic reaction involving an even-numbered ring. We assume that the alternant property is retained throughout, there being no interactions between AO's of atoms in the pericyclic ring other than between nearest neighbors, *i.e.*, those implied either in the valence structure of the reactant or in that of the product. The course of such a pericyclic reaction involving an even-numbered ring is topologicially equivalent to, or isoconjugate with, the interconversion of two classical (Kekulé) structures for an analogous cyclic polyene.[6] The two classical polyenes (R and S) and the intermediate hybrid (RS) can be derived by union[7] of methyl with an odd AH alternant hydrocarbon[7] (T) derived from R, S, or RS by loss of one carbon atom; *i.e.*

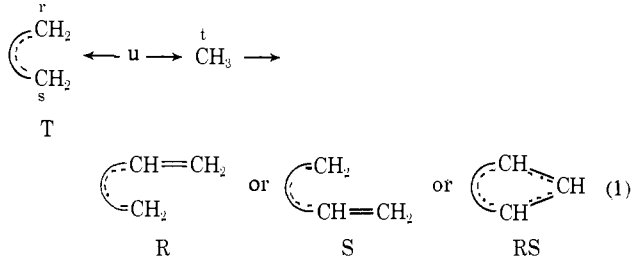

R S RS (1)

The HOMO and LUMO arise[7] in each case from an interaction between the NBMO of T and the 2p AO of methyl, the HOMO–LUMO splitting, ΔE, being given by

$$\Delta E = 2|(a_{or}\beta_{rt} + a_{os}\beta_{st}) \quad (1)$$

where a_{oi} is the NBMO coefficient at atom i in T, β_{ij} is the ij resonance integral, and the lettering of atoms is as indicated in eq 1.

In the case of a "forbidden"[8] pericyclic reaction, the AH RS isoconjugate with the transition state is antiaromatic. In that case[7,9] a_{or} and a_{os} in eq 1 have opposite signs. Since the conversion of R to S *via* RS corresponds to a decrease in β_{rt} from its initial value (β_{rt}^0) to zero and a simultaneous increase in β_{st} from zero to its final value (β_{st}^0), at some point in the reaction $a_{or}\beta_{rt}$ must become equal to $-a_{os}\beta_{st}$ so that ΔE van-

(1) This work was supported by the Air Force Office of Scientific Research through Contract F44620-71-C-0119 and the Robert A. Welch Foundation through Grant F-126. The calculations were carried out using the CDC 6400/6600 computer at The University of Texas Computation Center.

(2) R. B. Woodward and R. Hoffmann, *Angew. Chem., Int. Ed. Engl.*, 8, 781 (1969).

(3) H. C. Longuet-Higgins and E. W. Abrahamson, *J. Amer. Chem. Soc.*, 87, 2045 (1965).

(4) R. B. Woodward and R. Hoffmann, *J. Amer. Chem. Soc.*, 87, 2046 (1965).

(5) M. G. Evans, *Trans. Faraday Soc.*, 35, 824 (1939).

(6) M. J. S. Dewar, *Angew. Chem., Int. Ed. Engl.*, 10, 761 (1971).

(7) M. J. S. Dewar, "The Molecular Orbital Theory of Organic Chemistry," McGraw-Hill, New York, N. Y., 1969.

(8) If the terms "allowed" and "forbidden" are used in this connection, it is well to put them in quotation marks because "forbidden" pericyclic reactions are not in fact truly forbidden. They merely occur less easily than analogous "allowed" processes. See ref 6.

(9) M. J. S. Dewar and H. C. Longuet-Higgins, *Proc. Roy. Soc., Ser. A*, 214, 482 (1952).